EVALUATION OF THE HYDRO-METEOROLOGICAL DROUGHT INFLUENCE ON "LAKE AREA BY REMOTE SENSING"

Muhittin Karaman[1], Emre Özelkan[2,3]

[1]Istanbul Technical University, Faculty of Mines, Geology Engineering Department, Istanbul/Turkey
[2]Çanakkale Onsekiz Mart University, Faculty of Architecture & Design, Department of Urban and Regional Planning, Canakkale / Turkey
[3]Çanakkale Onsekiz Mart University, Graduate School of Natural and Applied Sciences, Risk Management of Natural Disasters Program, Canakkale / Turkey

ABSTRACT

Drought, which expresses the lack of water, has been one of the most important problems in every period and is the most common cause of food shortages. The most effective fight against drought and its effects is possible with well-organized water resources management. This study examines the spatio-temporal changes and effects of drought in a dam lake together with in-situ hydro-meteorological and satellite remote sensing data. The study area was selected as Bakacak Dam Lake in Çanakkale province, Turkey. Hydro-meteorological data was obtained by in-situ dam lake level and area observation/measurements and meteorological stations used to produce the Standard Precipitation Index (SPI) and potential evapotranspiration (PET) from Thornthwaite. In order to determine the spatio-temporal change of dam lake area the normalized difference water index (NDWI) images derived from Landsat were used as remote sensing data. The study covers the period of 2011-2020 and was carried out according to the 12-month water year calendar. The results of the study shows that during the dry season in the lake, significant spatial changes occurred under the influence of hydro-meteorological conditions. The change in the lake level causes a linear change in the lake area and lake volume. A change in level of 17.75 meters results in a volume change of 58 hm3. 1 m change in lake level causes a 0.155 km2 change in the lake area and 1 km2 change in the

lake area creates a volume change of approximately 20.5 hm3. 1 mm change in the annual total precipitation causes a 7100 m2 change in the lake area. In years when the total annual precipitation is high, the lake area increases significantly. Heavy rains at the end of the dry period, especially in September, cause an increase in the lake area at the end of the dry period. Extremely wet or extremely drought conditions do not occur in the lake during the investigated period. The increase in the positive values of SPI (i.e. wet conditions) causes an increase in the lake area, while the increase in the negative values (i.e. dry conditions) causes a decrease in the lake area. Additionally, at low levels of PET, the lake area is high, and at high levels of PET, the lake area is low. Since the study area is in a closed basin structure and the wind is weak, SPI gives better results than PET, and not only drought but also human activities such as water consumption and irrigation are effective in the changes in the water availability of the dam.

Keywords: *Hydro-meteorological drought, SPI, PET, remote sensing, NDWI*

1. INTRODUCTION

Drought, which is one of the most severe and frequent extreme events with the effect of climate change, is a meteorological-based natural disaster that expresses the lack of water in a certain period (Özelkan and Karaman 2018). Drought progresses insidiously and slowly, its beginning and end very difficult to estimate, and worst of all, its impacts proceed extended period of time (Wilhite 2020). First of all, drought adversely influences natural resources such as water, agricultural land and forests which are vital for the continuation of life (Özelkan et al. 2019a). Especially in arid and semi-arid climatic regions, the increasing need for natural resources and excessive consumption caused by the increasing population have made the fight against drought more urgent than ever (Genç et al., 2011; Çamoğlu et al. 2018; Çakaroz et al. 2020).

Drought is basically a lack of water and is evaluated under four interrelated headings as meteorological, hydrological, agricultural and socio-economic. (Özfidaner et al 2018; Özelkan et al. 2019a). Meteorological drought is the first stage that begins with a lack of precipitation and is the main and natural cause of all drought phenomena (Özelkan

and Karaman 2018; Mishra and Singh 2010). Hydrological drought is the second stage and expressed as the scarcity of underground and surface water resources fed by precipitation (Mishra and Singh 2010; Kapluhan 2013; Özelkan et al. 2019a). Agricultural drought is the third stage and refers to unfavorable conditions such as increase in diseases and deaths and decrease in production and yield due to lack of precipitation and water resources (Mishra and Singh 2010; Kapluhan 2013; Özelkan et al. 2016). Socio-economic drought is the last and most complex stage and is the reflection of meteorological, hydrological and agricultural droughts on social and economic life such as unemployment, migration, economic depression, unrest, poverty, food insecurity (Mishra and Singh 2010; Kapluhan 2013; Özelkan et al. 2019a). Considering the climate change and its effects, every stage of drought should be carefully examined, modeled and necessary precautions should be taken according to current and future climatic conditions.

Sustainable integrated water resources management is of great importance for sustainable life. Combining data from different sources and platforms makes water resources management more successful (Karaman et al. 2015; Özelkan 2020). As it is the first and most critical stage, the determination of meteorological drought is necessary for well-organized water resources management. Meteorological drought indices provide great convenience to examine the relationship between the change in water mass and the drought (Mohammed and Scholz 2017). Besides more sophisticated methods such as Standard Precipitation Evapotranspiration Index (SPEI) (Vicente-Serrano et al. 2010), Reconnaissance Drought Index (RDI) (Tsakiris and Vangelis 2005) and Palmer Drought Severity Index (Palmer 1965), Standard Precipitation Index (SPI) (McKee et al. 1993) working only with precipitation data provides useful, practical and robust drought analysis (Cheval 2015). Hydrological drought, which is the related with meteorological drought, evapotranspiration and human activities such as daily consumption and agricultural irrigation, is determined by many methods such as water level measurements, hydro-meteorological calculations, empirical open water surface evaporation calculations, water balance and budget calculations, heat and mass transport, and energy balance (Gorjizade et al. 2014; Özelkan and Karaman 2018). Among these methods, Thornthwaite, which calculates evapotranspi-

ration, is one of the most preferred hydro-meteorological calculations methods due to its easy calculation and interpretation (Thornthwaite 1948; Lang et al. 2017). In recent studies, the relationship between changes in water bodies and drought is commonly determined by using in-situ measurements and remote sensing data together (Karaman et al. 2018; Özelkan et al. 2019b). The most well-known and common way to determine change in water bodies and hydrological drought is to make in-situ water level and flow measurements (Yıldız and Deniz 2005; Özelkan 2020). However, in-situ measurements may have limitations such as time, space and cost. Continuity of measurements is very important especially in arid and semi-arid climates, where seasonal, monthly and even daily changes of water bodies are significant (Özelkan et al. 2019b). At this point, remote sensing technologies, which can view wide areas at once, provide great convenience to obtain real data for water resources management (McFeeters 1996; Xu 2006; Kale and Acarlı 2019). Remote sensing from satellite, providing the rapid and detailed information of water bodies, is commonly used in detecting and modeling hydrological drought (Schultz and Engman 2012; Kale and Acarlı 2019). Image classification and water indices are some of the most preferred remote sensing methods for detecting water bodies (Ji et al. 2009; Du et al. 2014; Gürsoy and Altun 2019). Water indices generated from spectral bands of remote sensing data are the most preferred, effective and easy methods for water body detection (Feyisa et al. 2014; Karaman et al. 2015; Özelkan 2020). In more detail, water indices consist of algorithms that take into account the high reflectance of water in the visible region and the low reflectance in the infrared region (McFeeters 1996; Xu 2006). McFeeter's (1996) the normalized difference water index (NDWI) considering green and near infrared (NIR) regions and Xu's (2006) the modified NDWI (MNDWI) considering green and short-wave infrared (SWIR) are among the most preferred and easily applied water indices, although there are more sophisticated methods such as the automated water extraction index (AWEI) (Feyisa et al., 2014) that work by considering the blue, green, NIR and SWIR regions. However, note that, previous studies show that associating remote sensing findings with meteorological and hydrological data makes remote sensing studies more significant and successful (Karaman et al. 2015, Özelkan and

Karaman 2018, Özelkan 2019).

In this study, the relationship between the spatio-temporal change of a dam lake area and drought was investigated. The Bakacak Dam Lake within the borders of Çanakkale City of Turkey was selected as the study area. The spatio-temporal change of the dam lake was determined using the NDWI from Landsat satellite images. The area values of water mass obtained by NDWI were verified with the water body area values calculated by using the in-situ measurements at the dam. The change in meteorological and hydrological drought in the region was determined by the SPI meteorological drought index and potential evapotranspiration (PET) from Thornthwaite method. The study covers the period of 2011-2020, all data acquisition and calculations were made according to the 12-month water year calendar. The findings show that NDWI is successful in determining the areal change and hydrological drought of the lake, and although meteorological drought is not effective alone, it is quite effective in the change in the lake area.

2. MATERIALS AND METHODS

2.1. Study Area

Bakacak Dam Lake is within Biga district of Çanakkale province in western Turkey and located between 26°55'00" - 27°01'27"E eastern meridians and 40°08'53" - 40°11'08" northern parallels and (Figure 1). Bakacak Dam Lake is used for multi-purposes such as for drinkable water, irrigation, fisheries, flood protection. The dam lake was built between 1991 and 1999 as a body of rock fill on Koca Çay Creek, situated 19 km from Biga District city center, 90 m above sea level and 65 m above riverbed (DSI 2021). The dam lake area and volume are 7.74 km^2 and 139 hm^3 at normal water level, respectively. The dam provides irrigation service to an agricultural area of 9,100 hectares (DSI 2021).

The region generally has a subtropical Mediterranean climate. In more detail, the study area is under the influence of the mild Marmara climate, which is the transition zone from the Black Sea to the Mediterranean. According to the data archive of the Turkish State Meteorological Service (MGM), the rainiest period is the end of autumn and the beginning of winter with a total monthly precipitation about 90 mm,

and the driest period is July with about 10 mm. Generally, winds blowing from the south bring precipitation, while winds blowing from the north cause low temperatures in winter to the region. Around the dam vicinity are generally found maquis elements that belongs to Mediterranean vegetation. Additionally, on the northern slopes of the dam are the species which grown under the effect of humid mild forests.



Figure 1. Study area

2.2. Meteorological Data and Pre-processing

The precipitation data measured at the meteorological station of MGM 21 km far from the dam were used to calculate SPI meteorological drought indices and potential evapotranspiration (PET) from Thornthwaite. All SPI and PET calculations were implemented according to the 12-month water year calendar that starts at the beginning of October and ends at the end of September. In other words, water year starts with the beginning of rainy season and ends with the end of dry season. The steps followed to calculate SPI are as follows: 1) Subtract the long-term average (X_m) from corresponding period's (X_i) precipitation total, and 2) Divide the difference you found in the first step by the standard deviation (σ) calculated from the long-term data (McKee et al. 1993; Dhakar et al. 2013; Özelkan et al. 2016).

$$SPI = (X_i - X_m)/\sigma \quad (1)$$

SPI can determine the amount of deviation of the meteorological values of a certain period from the climate values of long-term as 1, 3, 6, 9 and 12 month periods (Çakaroz et al. 2019). In this study, the SPI covering the 12-mont water year is expressed as SPI-12. The negative values of SPI represent the drought conditions with less precipitation, while the positive values represent the rainy conditions without drought. The SPI drought classes and values are presented in Table 1.

Table 1. SPI drought classes and values (Lu et al. 2021).

Drought Class	Drought Values
Extremely wet	≥2
Severely wet	1.5≤SPI≤1.99
Moderately wet	1.0≤SPI≤1.49
Normal	-0.99≤SPI≤0.99
Moderate drought	-1.49≤SPI≤-1.00
Severe drought	-1.99≤SPI≤-1.5
Extreme drought	≤-2.00

Thornthwaite method, where the primary target is climate classification, is frequently used in cases where evapotranspiration cannot be determined directly, especially in studies such as agriculture, hydrogeology, and water resources management (Thornthwaite 1948; Karaman et al. 2018). Thornthwaite method, which was stated to not give the satisfactory results in arid and excessively humid conditions (Pereira and Pruitt 2004), was preferred because Çanakkale has a mild climate. The potential evapotranspiration (PET) are determined by the Thornthwaite method as follows (Karaman et al. 2015).

$$i = \left(\frac{t}{5}\right)^{1,514} \rightarrow I = \sum_{k=1}^{12} i \rightarrow PET = 16 \times \left(\frac{10 \times t}{I}\right)^{a} \times G \quad (2)$$

$$a = (0.000000675 \times I^3) - (0.000077 \times I^2) + (0.01792 \times I) + 0.49239$$

Terms in equations are as follows: i = monthly temperature index, t = monthly mean temperature (°C), I = annual temperature index, PET = potential evapotranspiration (mm), a = coefficient, G = latitude correction coefficient (read from Thornthwaite chart).

2.3. Remote Sensing Data and Pre-Processing

A total of 8 Landsat images with 30 m spatial resolution were used between 2011 and 2020 from the data portal of United States Geological Survey (USGS) (Table 2). Since the satellite images will be associated with the SPI drought index values, Landsat images dated the end of the water year were preferred. In addition, atmospheric and geometric corrections of all surface reflectance images were performed by the vendor USGS. The NDWI water index, which works by considering the high reflectance of the water in the visible region and the low reflectance in the infrared (McFeeters 1996), was chosen to determine the water body area of the area. NDWI values range from -1 to 1 and above 0 indicates water (McFeeters 1996). NDWI were produced using the second and fourth bands of Landsat 5 Thematic Mapper (TM) and the third and fifth bands of Landsat 8 Operational Land Imager (OLI) instead of green and NIR in Equation 3 where R means reflection. The NDWIs for Landsat 5 TM and Landsat 8 OLI were represented in Equations 4 and 5 with the center wavelengths in micrometers, respectively:

$$NDWI = \frac{(R_{Green} - R_{NIR})}{(R_{Green} + R_{NIR})} \quad 3$$

$$NDWI_{Landsat\ 5\ TM} = \frac{(R_{0.5690} - R_{0.8400})}{(R_{0.5690} + R_{0.8400})} \quad 4$$

$$NDWI_{Landsat\ 8\ OLI} = \frac{(R_{0.5613} - R_{0.8646})}{(R_{0.5613} + R_{0.8646})} \quad 5$$

Table 2. List of Landsat satellite images used in study.

No	Acquisition Date	Satellite	Path/Row
1	04.10.2011	Landsat 5 TM	181/032
2	09.10.2013	Landsat 8 OLI	182/032
3	10.09.2014	Landsat 8 OLI	182/032
4	01.10.2016	Landsat 8 OLI	182/032
5	04.10.2017	Landsat 8 OLI	182/032
6	05.09.2018	Landsat 8 OLI	182/032
7	10.10.2019	Landsat 8 OLI	182/032
8	28.10.2020	Landsat 8 OLI	182/032

3. RESULTS

3.1. Long-Term Changes in the Lake Area Derived from Satellite Data

Satellite images were used for long-term monitoring of changes in the lake area. Binary raster images representing the water-covered area and the non-water area were produced by using the threshold value from the NDWI gray level image derived from the satellite images acquired at the end of September of different years. In the NDWI gray level image, binary images were produced so that pixels with a threshold value of zero and above represent water areas, and pixels with a value below the threshold value represent the non-water area class. By converting binary raster images to vector format, the lake shoreline or lake area vector on the date of each satellite image was obtained, and lake area information was created by calculating the area of the related vector.

At the end of September for the years 2011-2020, the lake areas were determined as the smallest 1.75 km^2 and the highest 4.60 km^2. At the end of September 2016, the lake area was at the smallest level, and at the end of September 2019, the lake area was at the largest level. Significant spatial changes have occurred in the lake in the same months of different years (Figure 2, Figure 3).

3.2. Relationship Between Lake Area, Lake Volume and Water Level

Changes in water level directly affect the lake area and lake volume (Figure 4). While the effect of level changes on the area is linear (R^2=0.964), the effect on the lake volume is exponential (R^2=0.991). The lake water level measured between 67.78 m and 85.63 m, and the lake volume ranged between 8.13 hm^3 and 66.43 hm^3, measured on the dates when satellite images were acquired at end of the September of 2011-2020 period. An area change of 1 km^2 in the lake area creates a volume change of approximately 20.5 hm^3 depending on the linear relationship between area and volume (R^2=0.987). A 1 m change in lake level causes a 0.155 km^2 change in the lake area. Between 68 m and 80 m elevations of the lake, 23.4 hm^3 of water is stored, and between 80 m and 85 m elevations, 30.6 hm^3 of water is stored.

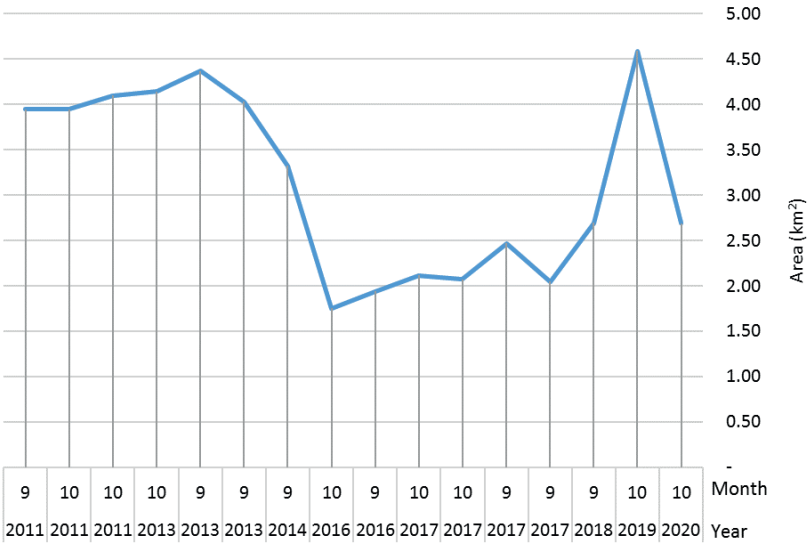


Figure 2. The long-term late September Lake area change graph

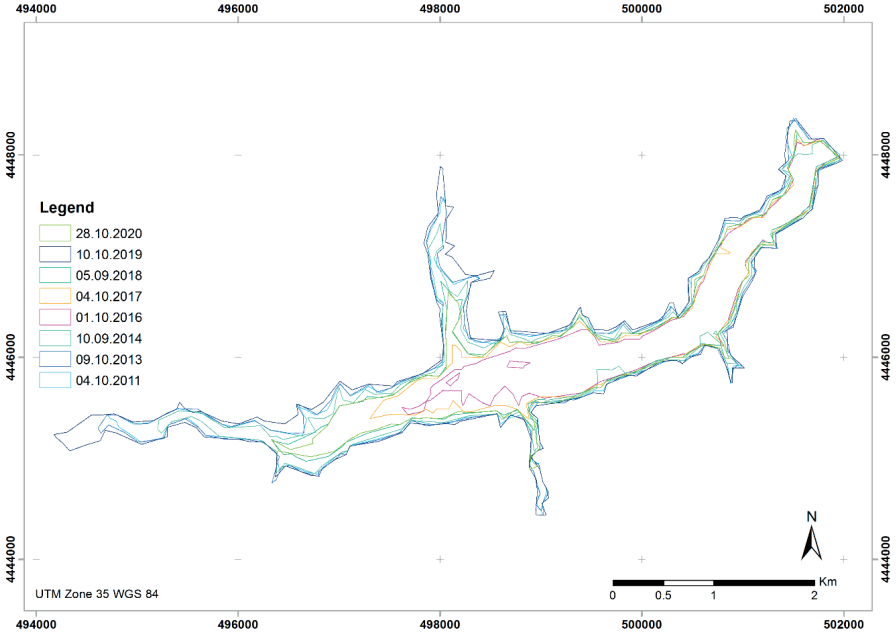


Figure 3. The long-term late September Lake area change map

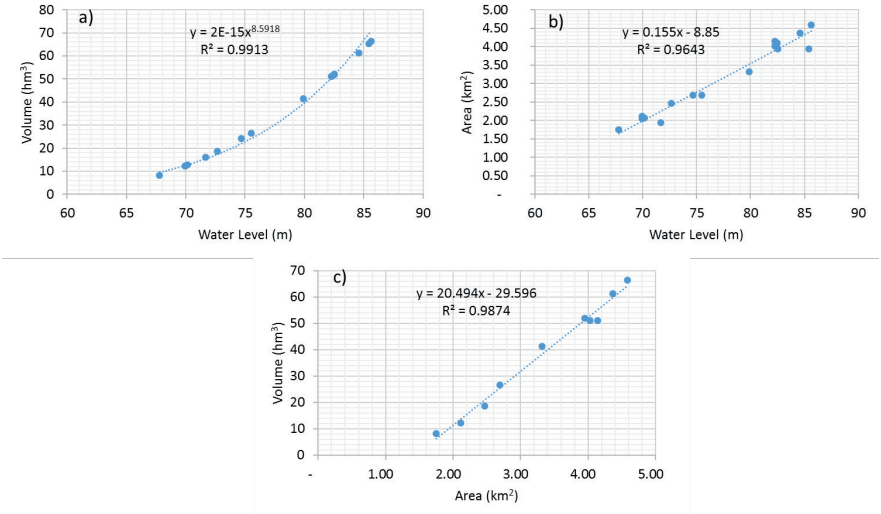


Figure 4. Scatter plots of volume-water level (a), area-water level (b) and volume-area (c) relationships

3.3. Long-Term Changes in Precipitation and Its Impact on the Lake Area

The effects of the total annual precipitation of the study area and the precipitation in September of each year on the lake area at the end of September of that year were evaluated separately. The annual total precipitation between 2011 and 2020 is between 511 mm and 816 mm. The highest amount of precipitation was 810 mm and 816 mm in 2018 and 2019, respectively, and the lowest amount of precipitation was 511 mm in 2020. The total precipitation in September for long-term varied between 0-125.4 mm. While the lowest level of precipitation occurred in September of 2011 (2.2 mm), 2019 (2.7 mm), and 2012 (3.8 mm), the highest level of precipitation occurred in September of 2014 (125.4 mm), 2018 (108.2 mm), and 2015 (57.9 mm) (Figure 5).

Total annual precipitation between 2011 and 2020 on the lake area is evaluated together for all years. As the total annual precipitation increases, the lake area also increases linearly (R^2=0.679). 100 mm change in the annual total precipitation causes a 0.71 km^2 change in the lake area (Figure 6).

When the effects of the September precipitation of 2011-2020 on the lake area are evaluated together for all years, it is also seen that two different trends are effective (Figure 7-a). Years of heavy precipitation (Figure 7-c) and years of low precipitation (Figure 7-b) are clustered in different regions in the total precipitation-area graph. The rainy months of September and the precipitation of around 25 mm directly affect the lake area at the end of September (Figure 7). Heavy rains in September contribute to the increase of the lake area (R^2=0.887). Since the excessive precipitation in September also contributes significantly to the total precipitation, a linear relationship develops between the September excessive precipitation and the area. In the periods when precipitation is extremely low in September, a negative correlation develops between precipitation and the lake area (R^2=0.706). It shows that the effect of September is low compared to the annual total precipitation in these periods and that the precipitation in September does not have a significant contribution to the total annual precipitation.

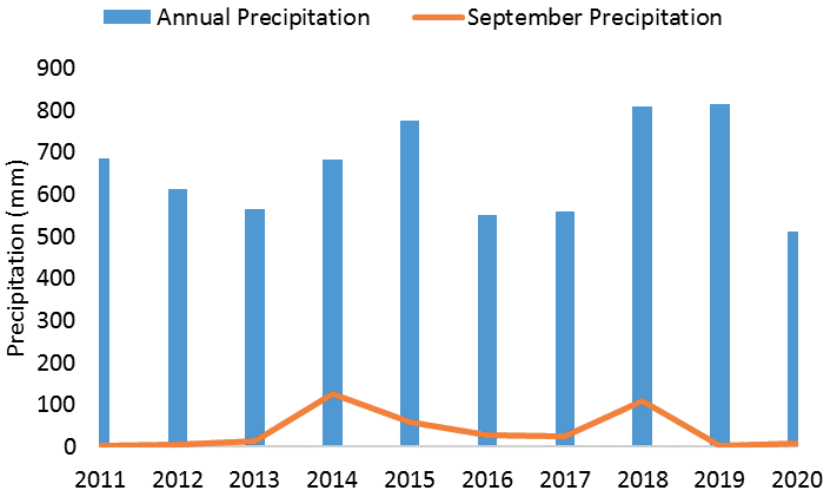


Figure 5. Total precipitation and precipitation in September for the years 2011-2020

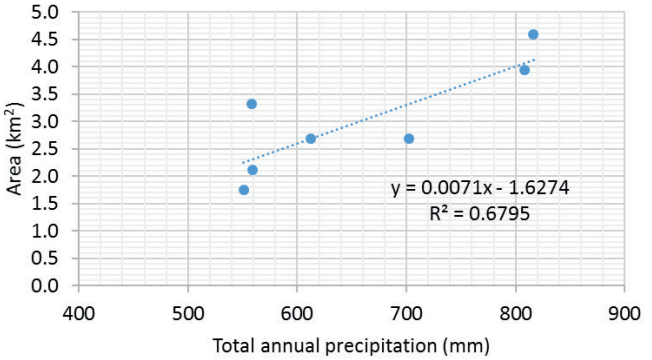


Figure 6. Scatter plot of the relationship between the total annual precipitation- area

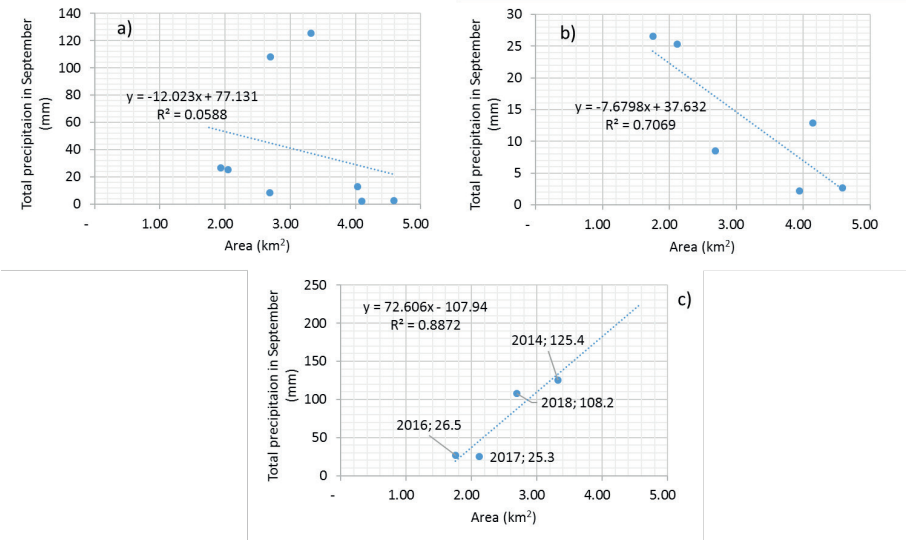


Figure 7. Scatter plot of the relationship between the area- total precipitation in September a) for all years b) for years of low precipitation c) for years of heavy precipitation

3.4. Area-SPI Relationship

Between 2011 and 2020, SPI values range from -1.117 to 1.337. The highest positive SPI value was in 2019, and the highest negative SPI value was in 2020. According to the SPI drought classification, 2019 is moderately wet and 2020 is moderately drought. In the examined years, extreme wet or extreme drought conditions did not occur. Except for 2019 and 2020, normal drought conditions were realized in the region according to SPI values (-0.745 to 0.385). During peri-

ods when SPI values are negative and arid conditions occur, the lake area becomes smaller (Figures 8). During periods when SPI values are positive and wet conditions occur, the lake area increases. A positive increase in SPI values causes a linear increase in the lake area, and an increase in SPI values in a negative direction causes a linear decrease in the lake area (R^2=0.508).

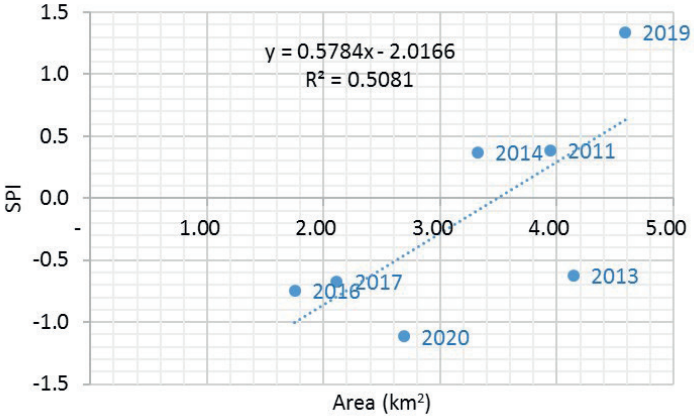


Figure 8. Scatter plot of the relationship between the area- SPI

3.5. Area-PET Relationship

PET values vary between 1012 mm and 1260 mm during the examination period. The highest levels of PET value were in 2020 with 1260 mm, and the lowest values were in 2011 with 2012 mm. The relationship between the area and PET values has a second-order polynomial or quadric model (R^2=0.43). The periods in which PET occurs at low levels are also the periods when the lake area is the highest. At the highest levels of PET the lake area is minimal (Figure 9).

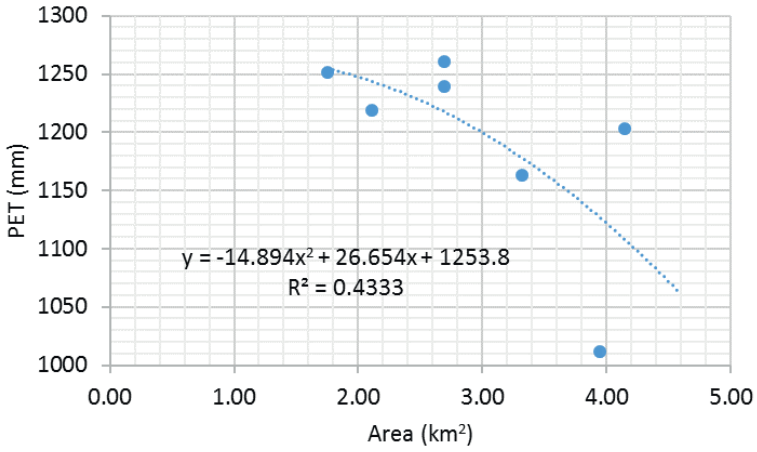


Figure 9. Quadric model of the Area-PET relationship

4. CONCLUSION

The increase in population, increase in pollution, decrease in resources, global warming and climate change have made water resources management one of the most important topics, especially for arid and semi-arid climate regions. Droughts triggered by climate change have become more frequent and more severe in recent years, and unfortunately, drought-affected areas are expected to increase gradually. Additionally, drought is the most common cause of food shortages, especially in developing countries. In this context, there is a need for an integrated and well-organized water resources management where data from different sources are used together.

The findings of this study show once again that the integrated use of in-situ hydro-meteorological measurements and remote sensing data makes water resources management more significant. Since the study area is in a closed basin structure and has weak winds, SPI have given better results than PET. Since the investigated reservoir is a dam lake, it can be said that drought is not the only determinant in the changes in the water body area, besides, human activities such as water consumption and irrigation are also effective. This study shows that remote sensing from satellite is a very effective tool in the management of water resources covering wide areas.

ACKNOWLEDGEMENTS

The authors would like to thank the USGS for the satellite images, the DSI for the hydrological data, the MGM for the meteorological data, and the Research Fund of Çanakkale Onsekiz Mart University for their support within the scope of Project 3253.

REFERENCES

Akçal, A., Demirel, K., Çamoğlu, G., (2017). Farklı Sulama Düzeylerinin Glayölde Korm Gelişimi ve Çiçeklerin Vazo Ömrü Üzerine Olan Etkileri, ÇOMÜ BAP FHD-2016-1031 No'lu Proje Sonuç Raporu.

Cheval, Sorin., (2015). The Standardized Precipitation Index – an overview. Romanian Journal of Meteorology. 12. 17-64.

Çamoğlu, G., Demirel, K., Genc, L., (2018) Use of infrared thermography and hyperspectral data to detect effects of water stress on pepper. Quantitative InfraRed Thermography Jour-nal, 15(1): 81-94.

Çakaroz, D., Özelkan, E., Karaman, M., (2020) Investigation of the effect of drought on tem-poral change in wetlands determined by remote sensing: The case study in Umurbey Delta (Çanakkale). European Journal of Science and Technology, (20), 898-916. DOI: 10.31590/ejosat.799717

Dhakar, R., Sehgal, V.K., Pradhan, S., (2013) Study on inter-seasonal and intra-seasonal relationships of meteorological and agricultural drought indices in the Rajasthan State of India. Journal of Arid Environments, 97: 108-119.

DSI (Turkish State Hydraulic Works), http://www2.dsi.gov.tr/baraj/baraj_arama.cfm. Acquisition date: 01.06.2021

Du, Z., Li, W., Zhou, D., Tian, L., Ling, F., Wang, H., Gui, Y., Sun B., Analysis of Landsat-8 OLI Imagery for Land Surface Water Mapping, Remote Sensing Letters, 5-7 (2014) 672-681.

Feyisa, G.L, Meilby, H., Fensholt, R., Proud, S.R., (2014) Automated water extraction index: A new technique for surface water mapping using Landsat imagery. Remote Sensing of Envi-ronment, 140: 23-35.

Genc, L., Demirel, K., Çamoglu, G., Asik, S., Smith, S., (2011) Determination of plant water stress using spectral reflectance measurements in watermelon (Citrullus vulgaris). American-Eurasian Journal of Agricultural & Environmental Sciences, 11(2): 296-304.

Gürsoy, Ö., Altun, R., (2019) Investigating surface water pollution by integrated remotely sensed and field spectral measurement data: A case study, Polish Journal of Environmental Studies, 28-4, 2139-2144.

Gorjizade, A., Akhondali, A.M., Zarei, H., Seyyed Kaboli, H., (2014) "Evaluation of Eight Evaporation Estimation Methods in a Semi-arid Region (Dez reservoir, Iran)", International Journal of Advanced Biological and Biomedical Research, 2(5), 1823-1836.

Ji, L., Zhang, L., Wylie, B., (2009) Analysis of Dynamic Thresholds for the Normalized

Difference Water Index, Photogrammetric Engineering & Remote Sensing, 75-11 1307–1317.

Kale, S., Acarlı, D., (2019) Shoreline change monitoring in Atikhisar reservoir by using re-mote sensing and geographic information system (GIS). Fresenius Environmental Bulletin, 28(5): 4329-4339.

Kapluhan, E., (2013) Drought and drought in turkey effect of agriculture. International Jour-nal of Geography and Geography Education, 27: 487-510.

Karaman, M., Budakoglu, M., Uca Avci, Z.D., Özelkan, E., Bülbül, A., Civas, M., Tasdelen, S., (2015) Determination of seasonal changes in wetlands using CHRIS/Proba hyperspectral satellite images: A case study from Acigöl (Denizli), Turkey. Journal of Environmental Biology, 36: 73-83.

Karaman, M., Özelkan, E, Taşdelen, S., (2018). Dar Nehirlerin Sentinel2-A Uydu Görüntüleri ile Belirlenebilirliğinde Havza Hidrojeolojisinin Etkisi: Karamenderes (Çanakkale) Örneği . Doğal Afetler ve Çevre Dergisi , 4 (2) , 140-155 . DOI: 10.21324/dacd.416514

Lang, D., Zheng, J., Shi, J., Liao, F., Ma, X., Wang, W., Chen, X., Zhang, M., (2017) A comparative study of potential evapotranspiration estimation by eight methods with FAO Penman-Monteith method in Southwestern China. Water, 9(10)734: 1-18.

Liu, C., Yang, C., Yang, Q., Wang, J., (2021) Spatiotemporal drought analysis by the standardized precipitation index (SPI) and standardized precipitation evapotranspiration index (SPEI) in Sichuan Province, China. Sci Rep 11, 1280. https://doi.org/10.1038/s41598-020-80527-3

McKee, T.B., Doesken, N.J., Kleist, J., (1993). The relationship of drought frequency and duration to time scales. Proceedings of the 8th Conference on Applied Climatology: Ameri-can Meteorological Society: 17-22 January 1993, Boston, MA, USA.

McFeeters, S.K., (1996) The use of normalized difference water index (NDWI) in the delinea-tion of open water features. International Journal of Remote Sensing, 17(7): 1425-1432.

Mishra, A.K., Singh, V.P., (2010) A review of drought concepts. Journal of Hydrology, 391(1-2): 204-216

Mohammed, R., Scholz, M., (2017). The reconnaissance drought index: a method for detect-ing regional arid climatic variability and potential drought risk. J. Arid Environ. https://doi.org/10.1016/j.jaridenv.2017.03.014

Özelkan, E., Chen, G., Üstündağ, B.B., (2016) Multiscale object-based drought monitoring and comparison in rainfed and irrigated agriculture from Landsat 8 OLI imagery». International Journal of Applied Earth Observation and Geoformation, 44: 159-170. https://doi.org/10.1016/j.jag.2015.08.003.

Özelkan, E, Karaman, M., (2018) The Analysis of the effect of meteorological and hydrologi-cal drought on dam lake via multitemporal satellite images: A case study in Atikhisar Dam Lake (Çanakkale). Omer Halisdemir University Journal of Engineering Sciences, 7(2): 1023-1037. DOI: 10.28948/ngumuh.443230.

Özelkan, E., (2019a) Evaluation of temporal change of dam lake area determined by remote sensing with meteorological drought: A case study in Atikhisar Dam

(Çanakkale). Turkish Journal of Agricultural and Natural Sciences, 6 (4), 904-916. DOI: 10.30910/turkjans.633634

Özelkan, E., (2019b). Comparison of remote sensing classification techniques for water body detection: A case study in Atikhisar Dam Lake (Çanakkale). Cumhuriyet Science Journal, 40 (3), 650-661. DOI: 10.17776/csj.556440

Özelkan, E., (2020) Water body detection analysis using NDWI indices derived from Land-sat-8 OLI. Polish Journal of Environmental Studies, 29(2), 1759-1769. https://doi.org/10.15244/pjoes/110447

Özfidaner, M., Şapolyo, D., Topaloğlu, F., (2018). Seyhan Havzası Akım Verilerinin Hidrolojik Kuraklık Analizi . Toprak Su Dergisi , 7 (1) , 57-64 . DOI: 10.21657/topraksu.410140

Palmer, W.C., (1965) Meteorological drought. Office of Climatology Research Paper 45, Weather Bureau, Washington, D.C., 58 pp.

Schultz, G.A., Engman, E.T., (2012) Remote sensing in hydrology and water management. Springer-Verlag Berlin Heidelberg, Berlin, Almanya, p. 483.

Tsakiris, G., Vangelis, H., (2005) Establishing a drought index incorporation evapotranspiration Eur. Water, 9 (10), pp. 3-11

Vicente-Serrano, S.M., Beguería, S., López-Moreno, J.I., (2010) A multi-scalar drought index sensitive to global warming: the standardized precipitation evapotranspiration index – SPEI. J. Clim. 23: 1696–1718.

Wilhite, D, A., (2000) Drought: A Global Assessment, Vol. I, edited by Donald A. Wilhite, chap. 1, pp. 3–18 (London: Routledge, 2000). http://digitalcommons.unl.edu/droughtfacpub/69

Xu, H., (2006) Modification of normalized difference water index (NDWI) to enhance open water features in remotely sensed imagery. International Journal of Remote Sensing, 27(14): 3025-3033.

Yıldız, M.Z., Deniz, O., (2005) The impacts of the level changes in closed basin lakes on the coastal settlements: The lake Van example. Fırat University Journal of Social Science, 15(1): 15-31.